

Manganese diffusion in monocrystalline germanium

A. Portavoce,^{a,b,*} O. Abbes,^{b,c} Y. Rudzevich,^d L. Chow,^d V. Le Thanh^c
and C. Girardeaux^b

^aCNRS, IM2NP, Faculté des Sciences de Saint-Jérôme case 142, 13397 Marseille, France

^bAix-Marseille Université, IM2NP, Faculté des Sciences de Saint-Jérôme case 142, 13397 Marseille, France

^cCNRS, CINAM, Campus de Luminy Case 913, 13288 Marseille, France

^dDepartment of Physics, University of Central Florida, Orlando, FL 32816, USA

Received 21 March 2012; revised 24 April 2012; accepted 27 April 2012

Available online 3 May 2012

The diffusion of a half monolayer of Mn deposited by molecular beam epitaxy on a Ge(001) substrate was studied via secondary ion mass spectrometry. Mn diffused in Ge under extrinsic conditions, exhibiting a solubility of 0.7–0.9%. All the Mn atoms were activated, occupying Ge substitutional sites and exhibiting a negative charge, in agreement with semiconductor doping theory. The diffusion mechanism being vacancy (*V*)-mediated, the formation of Mn–*V* pairs is suggested. Mn surface desorption occurred for temperatures >600 °C.

© 2012 Acta Materialia Inc. Published by Elsevier Ltd. All rights reserved.

Keywords: Mn; Diffusion; Ge; Spintronics

Interesting results concerning the magnetic properties of Mn-doped Ge structures have been reported [1–5]. Two types of Mn:Ge spintronic applications are currently being investigated: (i) the fabrication of a Mn-doped Ge diluted magnetic semiconductor (DMS), exhibiting tunable magnetic properties due to the use of electric field [1,3]; and (ii) the fabrication of a ferromagnetic Mn₅Ge₃ layer in epitaxy on Ge(111) [5–8], which could be used as an electric contact for spin injection in monocrystalline Ge. Thus, understanding Mn atom incorporation in Ge bulk is currently of great interest, since it raises many important theoretical issues. It is currently accepted that, in Ge, substitutional Mn atoms are double acceptors, promoting p-type doped Ge, while interstitial Mn atoms are donors that compensate both holes and magnetic moments due to substitutional Mn [9–11]. Mn-doped Ge films exhibit anomalous Hall effects [10,12], and the concentration of holes resulting from the activation of Mn doping atoms in Ge has been suggested to be a critical parameter driving the magnetic properties of Mn-doped Ge films [12]. In general, metallic impurities occupy substitutional sites in Ge [13–15]. In contrast to Si, in which

no significant substitutional Mn atoms can be found [10,16], experiments and calculations show that the concentration of substitutional Mn in Ge is higher than that of interstitial Mn [17,18]. Understanding of the electrical and magnetic properties of Mn:Ge DMS film relies on the knowledge of parameters that have not yet been well established. For example, the solubility of Mn in Ge is not really known, varying from 0.2 to 6% in the literature [3,11,12,18]. The proportion of substitutional Mn vs interstitial Mn is still under debate, and the charge of substitutional Mn ions is not clear. Mn can have different positive or negative charge states in Ge [9,11], but substitutional Mn²⁺ ions have been suggested [10,12,17]. Mn atoms were shown to exhibit a cluster tendency in Ge [19], and they appear to form complexes with Ge vacancies (Mn–*V* pairs) [15,20,21].

Mn diffusion experiments in Ge are interesting, as they can add to knowledge concerning Mn incorporation in Ge. Diffusion profiles can inform on Mn thermodynamic solubility (only mobile Mn atoms are in solution [22,23]). The determination of the Mn diffusion mechanism in Ge can give information concerning the proportion of substitutional and interstitial Mn [22,24–26], and high concentration (extrinsic) dopant diffusion informs about the charge of the substitutional dopant [22,24,26–28]. Dopant diffusion being dependent upon interactions between the dopant and point defects as

* Corresponding author at: CNRS, IM2NP, Faculté des Sciences de Saint-Jérôme case 142, 13397 Marseille, France. E-mail: alain.portavoce@im2np.fr

vacancies (V) and self-interstitials (I), the diffusion mechanism can also inform about dopant-point defects pairing [22,24,26–28]. Furthermore, the knowledge of the Mn diffusion coefficient in Ge is important for understanding and designing fabrication processes to produce relevant Mn:Ge structures, since different structures can be produced, such as nanocolumns [4,29], clusters [4,30], nano-films [3,5,31] and quantum dots [32]. In Si, Mn diffusion is direct interstitial [33], meaning that all diluted Mn atoms occupy interstitial sites. In Ge, the vacancy-mediated mechanism seems to prevail, since, in contrast to Si [22,24], Ge self-diffusion is vacancy-mediated only [25,34,35], as well as the diffusion of several dopants such as P and As [26–28], which are simultaneously using the interstitial and vacancy mechanisms in Si [24]. Regarding dopants, only B has been reported to use an interstitial-mediated mechanism in Ge [36,37].

This paper reports on Mn diffusion experiments in monocrystalline Ge. The sample was prepared in a molecular beam epitaxy (MBE) chamber exhibiting a residual pressure P of $\sim 1 \times 10^{-10}$ torr. Before loading in the MBE system, an Sb-doped Ge(001) substrate with resistivity $0.34 \Omega \text{ cm}$ was ex situ cleaned following a two-step procedure: (i) the sample was rinsed in various solvents using ultrasound; and (ii) the Ge native oxide was removed using a diluted HF solution. Once inside the MBE chamber, the Ge substrate was kept at $T = 450 \text{ }^\circ\text{C}$ for several hours, before heating to $750 \text{ }^\circ\text{C}$ for a few seconds. Once back to room temperature, a 0.5 atomic monolayer of Mn was deposited on the Ge substrate, using a standard effusion cell. Then, the sample was heated at $250 \text{ }^\circ\text{C}$ for 3 h to form the initial Mn diffusion source in the surface vicinity. Subsequently, the sample was removed from the MBE system and cut into $1 \times 1 \text{ cm}^2$ pieces. Thus, each of these sample pieces was annealed separately in a furnace under vacuum ($P < 7.5 \times 10^{-8}$ torr) at different T (from 450 to $750 \text{ }^\circ\text{C}$) and for different times t . Finally, Mn diffusion profiles in the annealed samples were measured by secondary ion mass spectrometry (SIMS), using an ADEPT 1010 Dynamic SIMS system operated at 2 kV with an O_2^+ primary ion beam with an impact angle of 40° compared with the normal of the sample surface. The raster area was $300 \times 300 \mu\text{m}^2$, with a detection window of $95 \times 95 \mu\text{m}^2$. In order to minimize the error on Mn diffusion lengths, the SIMS profiles were corrected following the method described in Ref. [38]. Using the as-deposited sample, the mixing-induced slope in the SIMS profiles in the analysis conditions was found to be 4.91 nm/decade (see Ref. [38]). The sample fabrication ensures equilibrium Mn diffusion since, in contrast to ion implantation, point defect supersaturation in Ge bulk is prevented. Consequently, the diffusion model used to extract diffusion coefficient in this work is based on thermodynamic equilibrium conditions.

Figures 1 and 2 present the SIMS profiles measured after annealing at 450 (192 h), 500 (50 h), 550 (5 h), 600 (1 h), 650 (1 h), 700 (1 h), and $750 \text{ }^\circ\text{C}$ (1 h). Mn diffusion profiles can be observed for temperatures up to $600 \text{ }^\circ\text{C}$. For higher temperatures, the samples were losing Mn during annealing (Fig. 2), owing to Mn surface desorption. Figure 1 shows that the maximum concentration of mobile Mn is $\sim 3\text{--}4 \times 10^{20} \text{ cm}^{-3}$, which corresponds

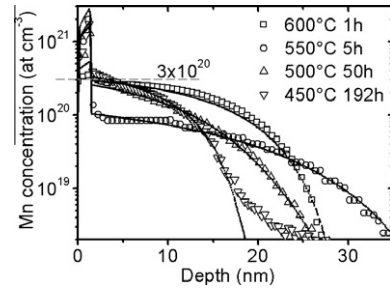


Figure 1. SIMS profiles measured after annealing (open symbols) and corresponding simulations used to extract the diffusion coefficients D_0 and D_1 (solid lines).

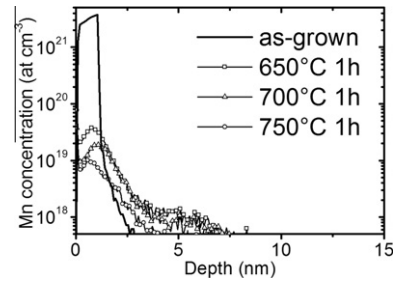


Figure 2. As-grown SIMS profile (solid line), with the SIMS profiles measured after annealing at 650 , 700 and $750 \text{ }^\circ\text{C}$ for 1 h (profiles not corrected, open symbols).

to a solubility limit of $0.7\text{--}0.9 \text{ at.}\%$. This is in agreement with the work of Ferri et al. [31] showing that the resistivity of Mn:Ge films decreases if the Mn concentration is $>1\%$, owing to the formation of clusters of Mn–Ge compounds. The diffusion profiles in Figure 1 do not correspond to the classical Fick diffusion. These types of dopant profiles are well known in semiconductors [22,24,26–28]; they are the result of both (i) an extra internal electric field driving force due to the coulomb interactions between the substitutional ionized (activated) dopants and the delocalized charge carriers (electrons or holes), and (ii) the variation in the dopant diffusion coefficient with concentration as a result of the variation in charge point defects with the semiconductor Fermi level. In the present case, Mn is known to act as a double acceptor in Ge and to generate holes [9–12]. Consequently, the Mn diffusion coefficient will be dependent on the local concentration of positively charged point defects, and thus dependent on the local hole concentration h [22,24]. In order to take into account the internal electric field between the activated dopants and the delocalized charged carriers, the diffusion flux J of dopants on substitutional sites exhibiting a charge q , can be written

$$J = -D \left(\frac{n}{n_i} \right)^{-q} \frac{d}{dx} \left(C \left(\frac{n}{n_i} \right)^{+q} \right) \quad (1)$$

with D the diffusion coefficient, C the dopant concentration, n the electron concentration, and n_i the intrinsic electron concentration in the semiconductor ($nh = n_i^2$). In general, the experimental profiles shown in Figure 1 can be obtained only if the interactions between the delocalized holes and the Mn substitutional ions are attractive (cooperation between the internal field driving

force and the concentration gradient driving force). Thus, substitutional Mn atoms have to exhibit a negative charge, and have to obey the charge balance equation $C + n = |q|h$ as for the general case of p-type dopants. Thus, the local concentration of holes in Ge is given by $h = (C + \sqrt{\alpha})/2|q|$ with $\alpha = C^2 + 4|q|n_i^2$, and the Mn flux is

$$J = -D_{\text{eff}} \left(1 + \frac{|q|C}{\sqrt{\alpha}} \right) \frac{dC}{dx} \quad (2)$$

Mn being a double acceptor in Ge [9,11], $q = -2$ is set in the present model (Mn²⁻ as substitutional ions). The variation in the effective Mn diffusion coefficient D_{eff} with concentration was set as [22,24]

$$D_{\text{eff}} = D_0 + D_1 \frac{h}{n_i} \quad (3)$$

D_0 corresponds to Mn diffusion using uncharged point defects, for which their concentration does not vary with the Ge Fermi level, and D_1 corresponds to Mn diffusion using point defects exhibiting a single (elementary) positive charge [22,24]. A third coefficient taking into account the use of double charged positive defects could be added ($D_2 \times h^2/n_i^2$) [22,24,26–28,36]. However, the simulations showed that the fit of the experimental profiles is not improved by doing so. In order to fit SIMS profiles correctly, it was necessary to take into account the presence of Mn clusters on the Ge surface for concentrations higher than a solubility limit of $4 \times 10^{20} \text{ cm}^{-3}$, as well as the dissolution of part of these clusters during diffusion. The diffusion equation used to model the Mn diffusion was then

$$\frac{dC}{dt} = -\frac{dJ}{dx} + k_{\text{cl}}C_{\text{cl}} \quad (4)$$

with k_{cl} the dissolution rate of the clusters, and C_{cl} the concentration of Mn atoms in the clusters. In the simulations, all the mobile Mn atoms were considered to be activated. n_i vs temperature was taken from the same source as in Ref. [27]. Figure 1 presents as a solid line the simulation results used to extract the diffusion coefficients D_0 and D_1 at 450, 500, 550 and 600 °C. It can be noted that the profile measured at 450 °C presents a second slope for concentrations close to $9 \times 10^{19} \text{ cm}^{-3}$, which cannot be fitted by the chosen model. Since this phenomenon was observed at the lowest temperature only (8 days of annealing), it has been neglected. However, simulations show that the total profile could be simulated if a second diffusion mechanism independent of the one described by Eqs. (1)–(4), following the classical Fick equations, was taken into account. At 600 °C, the curvature of the simulated profile is slightly different from the curvature of the SIMS profile. This curvature results from the additional effects of D_0 and $D_1 \times h/n_i$ in Eq. (3). Thus, this difference may be explained by a value of n_i at 600 °C slightly different from the value expected by the law used in Ref. [27]. D_0 and D_1 are reported vs T_m/T in Figure 3 (open circles for D_0 and open squares for D_1), with T_m the melting temperature of Ge (or Si) and T the annealing temperature. They correspond to the Arrhenius laws $D_0 = 1.54 \times 10^{-3} \exp(-2.36 \pm 0.01 \text{ eV}/$

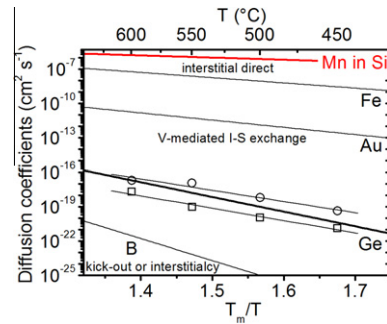


Figure 3. Comparison of diffusion coefficients of several species (Ge, Fe, Au and B) in Ge with the Mn coefficients measured in the present study (open circles for uncharged defects D_0 , and open squares for charged defects D_1). The diffusion coefficient of Mn in Si is also given (red thick solid line). Coefficients are given vs the ratio T_m/T , with T_m the melting temperature of the considered matrix (Ge or Si).

$kT) \text{ cm}^2 \text{ s}^{-1}$ and $D_1 = 1.29 \times 10^{-3} \exp(-2.60 \pm 0.01 \text{ eV}/kT) \text{ cm}^2 \text{ s}^{-1}$. k_{cl} was found to vary from $1.55 \times 10^{-6} \text{ s}^{-1}$ at 450 °C to $7.7 \times 10^{-4} \text{ s}^{-1}$ at 600 °C, following the Arrhenius law $k_{\text{cl}} = 6.43 \times 10^8 \exp(-2.13 \pm 0.01 \text{ eV}/kT) \text{ s}^{-1}$. Usually, three groups of impurities can be defined, depending on their diffusion kinetic: (i) the fastest impurities are dissolved on interstitial sites and are using the interstitial mechanism—this is the case of Fe in Ge (Fig. 3); (ii) for intermediate diffusion kinetics, the impurities are dissolved on substitutional sites, but thanks to an interstitial–substitutional exchange mechanism, diffuse on interstitial sites, as Au in Ge (Fig. 3); and (iii) the slowest impurities that exhibit in general a diffusivity close to the matrix atom self-diffusion, usually using mechanisms similar to the matrix atoms, are dissolved on substitutional sites, but are using complex point defects as dopant–point defect pairs in order to diffuse, as As and P using As– V and P– V pairs in Ge [26–28,36]. Contrasting with Si, Ge self-diffusion is using vacancies only [25,34,35]. Consequently, impurities using self-interstitial-mediated mechanisms are predicted to exhibit diffusion kinetics significantly slower than Ge self-diffusion [28,39] (this is the case of B in Ge; Fig. 3), while vacancy-mediated impurities are predicted to exhibit diffusion kinetics closer to Ge self-diffusion (as As and P) [26–28,36]. Ge self-diffusion [35], as well as the diffusion of Fe [40], Au [13] and B [37] in Ge is presented in Figure 3 for comparison with the Mn diffusion measured in the present work. Similar to the case of As and P diffusion in Ge, the Mn diffusion coefficients are close to Ge self-diffusion, leading to the conclusion that Mn diffusion is vacancy-mediated in Ge. Mn diffusion is ~ 10 orders of magnitude slower in Ge than in Si (Fig. 3). Considering Eq. (3), the intrinsic Mn diffusion coefficient ($h/n_i = 1$) can be defined as $D_{\text{in}} = D_0 + D_1 = 1.72 \times 10^{-3} \exp(-2.37 \pm 0.01 \text{ eV}/kT) \text{ cm}^2 \text{ s}^{-1}$. It is interesting to note that the activation energy found for Mn (2.37 eV) is quite close to the activation energies of Sb (2.3 eV) measured by Kosenko [41], of As (2.4 eV) measured by Bösenberg [42] and of P (2.4 eV) measured by Dunlop [43], which all exhibit $X-V$ pair mediated diffusion. As formerly suggested [26,44], the difference in activation energy (E_a) between Ge self-diffusion (3.09 eV [35]) and $X-V$ -mediated impurity diffusion is related to the binding energy between the substitutional dopant X and the vacancy V in second or

third nearest-neighbor position. In the case of As, theoretical calculations predicted that the As–V pair binding energy in Ge should be equal to 0.68 eV [45], which is in good agreement with the value given by the experimental activation energies of Ge and As previously cited: $E_a^{\text{Ge}} - E_a^{\text{AsV}} = 3.09 - 2.4 = 0.69$ eV (Brotzmann and Bracht reported a lower value of 0.38 eV [26]). Consequently, in agreement with previous theoretical work [15,20,21], Mn diffusion in Ge appears to be mediated by Mn–V point defects, exhibiting a binding energy of 0.72 eV that is close to the P–V (0.69 eV from Ref. [43]), As–V (0.69 eV from Ref. [42]), and Sb–V (0.79 eV from Ref. [41]) binding energies (Brotzmann and Bracht reported the values of 0.24, 0.38 and 0.54 eV for P, As and Sb, respectively [26]).

In conclusion, Mn diffusion in monocrystalline Ge was studied under thermodynamic equilibrium and extrinsic conditions for temperatures between 450 and 600 °C. Experiments show that Mn diffusion is vacancy-mediated in Ge, and follows the classical behavior of p-type dopants. All the diluted Mn atoms occupy substitutional sites, and exhibit a negative charge and a solubility limit of 0.7–0.9%. In addition, the results suggest that substitutional Mn ions form Mn–vacancy pairs. Annealing at temperatures >600 °C under vacuum promotes Mn desorption from the Ge surface. The solubility limit reported in the present work suggests that the magnetic properties of annealed Mn:Ge “DMS” with Mn concentration >1% are actually related to magnetic Mn–Ge phase precipitation.

- [1] S. Cho, S. Choi, S.C. Hong, Y. Kim, J.B. Ketterson, B.-J. Kim, Y.C. Kim, J.-H. Jung, Phys. Rev. B 66 (2002) 033303.
- [2] F. Tsui, L. He, L. Ma, A. Tkachuk, Y.S. Chu, K. Nakajima, T. Chikyow, Phys. Rev. Lett. 91 (2003) 177203.
- [3] J.-P. Ayoub, L. Favre, I. Berbezier, A. Ronda, L. Morresi, N. Pinto, Appl. Phys. Lett. 91 (2007) 141920.
- [4] I.-S. Yu, M. Jamet, T. Devillers, A. Barski, P. Bayle-Guillemaud, C. Beigné, J. Rothman, V. Baltz, J. Cibert, Phys. Rev. B 82 (2010) 035308.
- [5] A. Spiesser, I. Slipukhina, M.-T. Dau, E. Arras, V. Le Thanh, L. Michez, P. Pochet, H. Saito, S. Yuasa, M. Jamet, J. Derrien, Phys. Rev. B 84 (2011) 165203.
- [6] S. Olive-Mendez, A. Spiesser, L.A. Michez, V. Le Thanh, A. Glachant, J. Derrien, T. Devillers, A. Barski, M. Jamet, Thin Solid Films 517 (2008) 191.
- [7] A. Spiesser, V. Le Thanh, S. Bertaina, L.A. Michez, Appl. Phys. Lett. 99 (2011) 121904.
- [8] M.-T. Dau, V. Le Thanh, T.-G. Le, A. Spiesser, M. Petit, L.A. Michez, R. Daineche, Appl. Phys. Lett. 99 (2011) 151908.
- [9] S.J. Pearton, Solid-State Electronics 25 (1982) 499.
- [10] W. Zhu, Z. Zhang, E. Kaxiras, Phys. Rev. Lett. 100 (2008) 027205.
- [11] M.C. Dolph, T. Kim, W. Yin, D. Recht, W. Fan, J. Yu, M.J. Aziz, J. Lu, S.A. Wolf, J. Appl. Phys. 109 (2011) 093917.
- [12] S. Zhou, D. Bürger, M. Helm, H. Schmidt, Appl. Phys. Lett. 95 (2009) 172103.
- [13] H. Bracht, N.A. Stolwijk, H. Mehrer, Phys. Rev. B 43 (1991) 14465.
- [14] P. Clauws, E. Simoen, Mater. Sci. Semicond. Process. 9 (2006) 546.
- [15] S. Decoster, S. Cottenier, B. De Vries, H. Emmerich, U. Wahl, J.G. Correia, A. Vantomme, Phys. Rev. Lett. 102 (2009) 065502.
- [16] S. Zhou, K. Potzger, Gufei Zhang, A. Mücklich, F. Eichhorn, N. Schell, R. Grötzschel, B. Schmidt, W. Skorupa, M. Helm, J. Fassbender, Phys. Rev. B 75 (2007) 085203.
- [17] A. Stroppa, G. Kresse, A. Continenza, Phys. Rev. B 83 (2011) 085201.
- [18] S. Picozzi, L. Ottaviano, M. Passacantando, G. Profeta, A. Continenza, F. Priolo, M. Kim, A.J. Freeman, Appl. Phys. Lett. 86 (2005) 062501.
- [19] A. Continenza, G. Profeta, S. Picozzi, Appl. Phys. Lett. 89 (2006) 202510.
- [20] S. Decoster, S. Cottenier, U. Wahl, J.G. Correia, L.M.C. Pereira, C. Lacasta, M.R. Da Silva, A. Vantomme, Appl. Phys. Lett. 97 (2010) 151914.
- [21] A. Continenza, G. Profeta, Phys. Rev. B 78 (2008) 085215.
- [22] P.M. Fahey, P.B. Griffin, J.D. Plummer, Rev. Mod. Phys. 61 (1989) 289.
- [23] A. Portavoce, P. Gas, I. Berbezier, A. Ronda, J.S. Christensen, A.Y. Kuznetsov, B.G. Svensson, Phys. Rev. B 69 (2004) 155415.
- [24] P. Pichler, Intrinsic Point Defects, Impurities, and their Diffusion in Silicon, Springer, New York, 2004.
- [25] R. Fischer, W.F.J. Frank, K. Lyutovich, Physica B 273–274 (1999) 598.
- [26] S. Brotzmann, H. Bracht, J. Appl. Phys. 103 (2008) 033508.
- [27] T. Canneaux, D. Mathiot, J.-P. Ponpon, Y. Leroy, Thin Solid Films 518 (2010) 2394.
- [28] H. Bracht, S. Brotzmann, Mater. Sci. Semicond. Process. 9 (2006) 471.
- [29] M. Rovezzi, T. Devillers, E. Arras, F. d’Acapito, A. Barski, M. Jamet, P. Pochet, Appl. Phys. Lett. 92 (2008) 242510.
- [30] Y. Wang, J. Zou, Z. Zhao, X. Han, X. Zhou, K.L. Wang, Appl. Phys. Lett. 92 (2008) 101913.
- [31] F.A. Ferri, M.A. Pereira-da-Silva, A.R. Zanatta, A.L.S. Varella, A.J.A. de Oliveira, J. Appl. Phys. 108 (2010) 113922.
- [32] F. Xiu, Y. Wang, J. Kim, A. Hong, J. Tang, A.P. Jacob, J. Zou, K.L. Wang, Nat. Mater. 9 (2010) 337.
- [33] D. Gilles, W. Bergholz, W. Schröter, J. Appl. Phys. 59 (1986) 3590.
- [34] G.L. McVay, A.R. DuCharme, Phys. Rev. B 9 (1974) 627.
- [35] M. Werner, H. Mehrer, H.D. Hochheimer, Phys. Rev. B 32 (1985) 3930.
- [36] C. Janke, R. Jones, J. Coutinho, S. Oberg, P.R. Briddon, Mater. Sci. Semicond. Process. 11 (2008) 324.
- [37] S. Uppal, A.F.W. Willoughby, J.M. Bonar, N.E.B. Cowern, T. Grasby, R.J.H. Morris, M.G. Dowsett, J. Appl. Phys. 96 (2004) 1376.
- [38] A. Portavoce, N. Rodriguez, R. Daineche, C. Grosjean, C. Girardeaux, Mater. Lett. 63 (2009) 676.
- [39] P. Delugas, V. Fiorentini, Phys. Rev. B 69 (2004) 085203.
- [40] A.A. Bugai, V.E. Kosenko, E.G. Miselyuk, Sov. Phys. Tech. Phys. (English Transl.) 2 (1957) 183.
- [41] V.E. Kosenko, Proc. Acad. Sci. USSR Phys. Ser. (English Transl.) 20 (1956) 1399.
- [42] W. Bösenberg, Z. Naturforsch. (a) 10 (1955) 285.
- [43] W.C. Dunlop Jr., Phys. Rev. 94 (1954) 1531.
- [44] S.T. Dunham, C.D. Wu, J. Appl. Phys. 78 (1995) 2362.
- [45] A. Choneos, R.W. Grimes, C. Tsamis, Mater. Sci. Semicond. Process. 9 (2006) 536.